RESEARCH   **Open Access**

A novel DOA estimation method for an antenna array under strong interference

Ming Zuo and Shuguo Xie*

*Correspondence:
xieshuguo@buaa.edu.cn

School of Electronic
and Information Engineering,
Beihang University,
Beijing 100191, China

Abstract

Strong interference will affect direction of arrival (DOA) estimation of weak desired signal and even cause DOA estimation failure. This paper investigates the weak signal DOA estimation for an antenna array under strong interference signals, and proposed a novel DOA estimation method for strong interference source suppression and weighted l_1-norm sparse representation. A parallel adaptive beamforming algorithm based on power inversion is used to suppress strong interference and form new array data. To reduce spurious peaks in the spectrum under strong interference, a weighted matrix is determined by the optimized subspace algorithm for the subspace projection. Then, the DOA estimation, which is calculated by weighted l_1-norm sparse representation, is formed by the weighted matrix and new array data. In this paper, the superiority of the proposed algorithm is illustrated by an example of unmanned aerial vehicle (UAV) video signal DOA estimation under strong interference signals. The simulated results of an orthogonal frequency division multiplexing signal indicate that the proposed algorithm shows merits of fewer snapshots, a sharper main lobe, a lower average noise spectrum value, higher DOA estimation accuracy and success rate. For validation, an outdoor experiment was conducted which demonstrated that the proposed algorithm is superior to other algorithms and can be used for DOA estimation of UAV video signals under strong WiFi interference. Both the simulations and experiments verify that the proposed algorithm can effectively suppress strong interference and achieve better DOA estimation performance for weak signals.

Keywords: Strong interference, Parallel adaptive beamforming, Weighted l_1-norm sparse representation, DOA estimation, UAV video signal

1 Introduction

In complicated electromagnetic environment, the strong interference signals can affect the direction of arrival (DOA) estimation of weak signals. For example, unmanned aerial vehicle (UAV) video signals work in the 2.4 GHz or 5.8 GHz industrial, scientific and medical (ISM) frequency band, which is often affected by the strong interference signals such as WiFi, Bluetooth and other interference signals [1–4]. When the amplitudes of the interference signals are small, the traditional spectral estimation or sparse representation algorithm can be used to estimate the DOA of multiple signals simultaneously [5–7]. If the amplitudes of the interference signal are much larger than the desired signal, the spectrum peak of weak signals may

be annihilated by either strong interference spectrum peaks or spurious peaks in the algorithm, which will significantly affect the DOA estimation of weak signals [8].

There are two DOA estimation methods for weak signals under strong interference: one is to separate and estimate strong and weak signals simultaneously, and the other is to suppress strong interference signals and then estimate the DOA of weak signals. For the first method, Li et al. [9] proposed the RELAX algorithm, which uses the concept of signal separation to divide the array data into multiple data blocks, and then estimate the DOA of the desired signal. Tsao et al. [10] proposed a signal separation algorithm based on CLEAN technology. This method is realized by an iterative technique, which requires considerable computation and is difficult to implement in practical applications. For the second method, the jamming jam method (JJM) was proposed based on the DOA estimation of the multiple signal classification (MUSIC) algorithm [11] by constructing a block matrix to form a new array data. Reference [12] improved the JJM algorithm to be suitable for arbitrary arrays. The method in [13] used weighted Bartlett beamforming, which divides the array into multiple subarrays. A null was formed in the interference space direction of these subarrays, and weighted subarrays were used to construct a new array for DOA estimation. In [14], the direction vector of strong interference was projected into an orthogonal subspace to eliminate interference. However, the above methods require the interference direction to be as a priori information. Therefore, the extended noise subspace (ENS) method was proposed in [15]. It combines the interference subspace with the noise subspace to form a new noise subspace, and then estimates DOA according to the MUSIC algorithm. An improved ENS for weak signal DOA estimation under strong interference and coloured noise was presented in [16]. Gong et al. [17] proposed a DOA estimation algorithm based on the elimination of the eigenvectors of interference (EEOI). The eigenvectors of the weak signals are determined by the ratio of the eigenvalues to eliminate interference, the noise subspace is reconstructed, and then the DOA of the weak signal is estimated by the MUSIC algorithm. These methods are effective in a certain range of signal-to-interference ratios (SIRs). However, when less than or greater than a certain SIR, the ratio of spectrum peak to the average noise spectrum value is small. This increases the spurious peak, which would not be conducive to the DOA estimation of weak signals. Yang et al. [18] proposed the sparse spectrum fitting-matrix filter algorithm and sparse spectrum fitting-matrix filter with the nulling algorithm [19] to suppress interference. These two algorithms require passband or stopband range as a priori knowledge, which is not applicable for blind DOA estimation in real-world scenarios.

This paper proposes a novel DOA estimation for strong interference source suppression and weighted l_1-norm sparse representation. A parallel adaptive beamforming algorithm based on power inversion (PI) is used to suppress interference and form new array data, and the weighted matrix is determined by the optimized subspace algorithm of the subspace projection. Then, the weighted l_1-norm sparse representation DOA estimation is formed by the weighted matrix and the new array signal data. The proposed algorithm does not require the interference direction as a priori knowledge, and has strong

adaptability to different SIRs. In addition, it can effectively suppress strong interference and achieve better DOA estimation performance for weak UAV video signal.

The remainder of this paper is organized as follows: Sect. 2. introduces the array signal model. Section 3 provides the DOA estimation method under strong interference, and Sect. 4. presents the effectiveness of the proposed method in simulation and real-world scenarios. Finally, Sect. 5 concludes this work.

Notation Vectors and matrices are shown in bold lowercase and bold uppercase, respectively. Symbols vec($\cdot$), $(\cdot)^T$ and $(\cdot)^H$ denote the matrix vec operator, transpose and conjugate transpose. The symbol $(\cdot)^*$ represents conjugation. The symbol $E(\cdot)$ denotes expectation. Symbols $||(\cdot)||_{l1}$ and $||(\cdot)||_{l2}$ denote the l_1-norm and l_2-norm of the vector, respectively.

2 Array signal model

Assume that K far-field narrowband desired signals and Q far-field narrowband strong interference signals impinge on a uniform linear array with M elements ($K + Q < M$), and the spacing of adjacent antenna elements is half wavelength. Then, the received signal of the *m*th element can be expressed as

$$x_m(t) = \sum_{k=1}^{K} \mathbf{a}(\theta_k)s_k(t) + \sum_{q=1}^{Q} \mathbf{a}\left(\theta_q\right)j_q(t) + n_m(t)(t = 1, 2 \cdots T) \tag{1}$$

where

$$\mathbf{a}(\theta_k) = \left[1, e^{-i2\pi d \sin \theta_k / \lambda}, \cdots, e^{-i2\pi (M-1)d \sin \theta_k / \lambda}\right]^T \tag{2}$$

$$\mathbf{a}\left(\theta_q\right) = \left[1, e^{-i2\pi d \sin \theta_q / \lambda}, \cdots, e^{-i2\pi (M-1)d \sin \theta_q / \lambda}\right]^T \tag{3}$$

where $\mathbf{a}(\theta_k)$ is the M × 1 steering vector of the desired signal, $\mathbf{a}(\theta_q)$ is the M × 1 steering vector of strong interference, d is the distance of the adjacent antenna elements, and λ is the signal wavelength. θ_k is the incident angle of the desired signal, θ_q is the incident angle of the desired signal, and T is the number of snapshots. $s_k(t)$ is the *k*th desired signal, $j_q(t)$ is the *q*th strong interference signal, and $n_m(t)$ is Gaussian random noise. The vector of Formula (1) can be represented as

$$\mathbf{X}(t) = \mathbf{A}_k(\theta)\mathbf{S}(t) + \mathbf{A}_q(\theta)\mathbf{J}(t) + \mathbf{N}(t) \tag{4}$$

where $\mathbf{X}(t) = [x_1(t), x_2(t), ..., x_M(t)]^T$, $\mathbf{A}_k(\theta) = [\mathbf{a}(\theta_1), \mathbf{a}(\theta_2), ..., \mathbf{a}(\theta_K)]$ is the M × K dimensional steering matrix of the desired signal, and $\mathbf{A}_q(\theta) = [\mathbf{a}(\theta_1), \mathbf{a}(\theta_2), ..., \mathbf{a}(\theta_Q)]$ is the M × Q dimensional steering matrix of the strong interference signal. $\mathbf{S}(t) = [s_1(t), s_2(t), ..., s_K(t)]^T$ and $\mathbf{J}(t) = [j_1(t), j_2(t), ..., j_Q(t)]^T$ are the K × T dimensional desired signal matrix and the Q × T dimensional strong interference signal matrix, respectively. $\mathbf{N}(t) = [N_1(t), N_2(t), ..., N_M(t)]^T$ is an additive white Gaussian noise matrix with zero mean and σ_n^2 variance. Formula (4) can be simplified as

$$\mathbf{X} = \mathbf{A}_k \mathbf{S} + \mathbf{A}_q \mathbf{J} + \mathbf{N} \tag{5}$$

3 Methods

Our goal is to estimate DOA of weak signals under strong interference. Based on the array signal model proposed in Sect. 2, the proposed method is illustrated in this section. Figure 1 presents the flow chart of the proposed algorithm. The parallel adaptive beamforming algorithm based on PI is applied to the received signal in Formula (3) to suppress strong interference and form new array data. To reduce the spurious peaks in the spectrum under strong interference, the weighted matrix is determined according to the optimized subspace algorithm of the subspace projection. Then, the DOA estimation, which is calculated by weighted l_1-norm sparse representation, is formed by the weighted matrix and new array data.

3.1 The parallel algorithm of adaptive beamforming based on PI

It can be seen in Sect. 1 that many interference suppression algorithms, such as DOA estimation, require prior knowledge, and the performance is affected by SIR. To suppress strong interferences in the mixed signal, we propose a parallel algorithm of adaptive beamforming based on PI. We assumed that the signal received by the first array element is used as the reference signal, and the weighted output of the remaining M-1 array elements is expressed as

$$\mathbf{y}_{1,M-1} = \mathbf{w}_{M-1}^H \mathbf{X}_{M-1} \tag{6}$$

In the above formula, $\mathbf{w}_{M-1} = [w_2, w_3, ..., w_M]^T$ is the weighted vector, and the signal of the 2nd to Mth array elements is $\mathbf{X}_{M-1} = [x_2, x_3, ..., x_M]^T$. According to the minimum mean square error criterion [20], the 2nd to Mth channel can be used as input to obtain the weighted matrix

$$\mathbf{w}_{M-1} = \mathbf{R}_b^{-1} \mathbf{R}_a \tag{7}$$

where $\mathbf{R}_b = E[\mathbf{X}_{M-1}\mathbf{X}H\,M\text{-}1]$ is the autocorrelation of the second to M array element data, and $\mathbf{R}_a = E[\mathbf{X}_{M-1} x_1^*]$ is the cross-correlation between the second to M array element data and the first array element data. Therefore, the optimal weighted vector under this model is

$$\mathbf{w}_{\text{opt1}} = \begin{bmatrix} 1 \\ \mathbf{w}_{M-1} \end{bmatrix} = \begin{bmatrix} 1 \\ \mathbf{R}_b^{-1}\mathbf{R}_a \end{bmatrix} \tag{8}$$
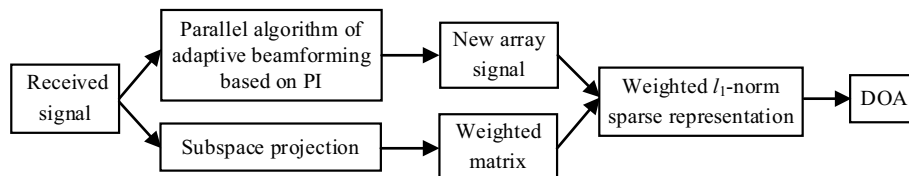

Fig. 1 Flow chart of the proposed algorithm

To obtain the best weight vector and update it in time, we use the least mean square algorithm to achieve adaptive weight calculation [21]; that is, the weight at time n + 1 is determined by the weight and correction number at time n. The adaptive weight is

$$\mathbf{w}_{M-1}(n+1) = \mathbf{w}_{M-1}(n) + \mu \mathbf{X}_{M-1}(n)\left[x_1(n) - \mathbf{w}_{M-1}^H(n)\mathbf{X}_{M-1}(n)\right]^*, \mu(0 < \mu < \mathrm{tr}(\mathbf{R}_b)) \tag{9}$$

where μ is the convergence factor, and the weighted output signal of M array elements can be expressed as

$$\mathbf{y}_1 = \mathbf{w}_{\mathrm{opt1}}\mathbf{X} \tag{10}$$

At this time, $\mathbf{y}_1$ is the signal vector after suppressing strong interference, but the signal vector cannot form a steering vector, which is unable be processed by spatial array signal processing. Therefore, the DOA estimation cannot be performed with $\mathbf{y}_1$. To solve this problem, we propose a parallel PI algorithm as shown in Fig. 2. One of the array elements is used as the reference signal and other M−1 array elements to solve the weight vector. Each of the reference array data and other M−1 array data are substituted into Eqs. (6)–(10) to obtain the new M-channel data $\mathbf{Y} = [\mathbf{y}_1, \mathbf{y}_2, ..., \mathbf{y}_M]^{\mathrm{T}}$ after interference suppression. For the reference array data, $\mathbf{w}_{\mathrm{optm}}$ is a fixed constant ($m = 1, ..., M$), so the phase of $\mathbf{y}_M$ is the same as original signal $\mathbf{x}_m$ according to Eq. (10). That is, the spatial processing cannot change the phase of the original signal, and the phase of the original signal is basically unchanged after the M-line parallel PI algorithm. Therefore, the output signal can be used as the input for subsequent DOA estimation.
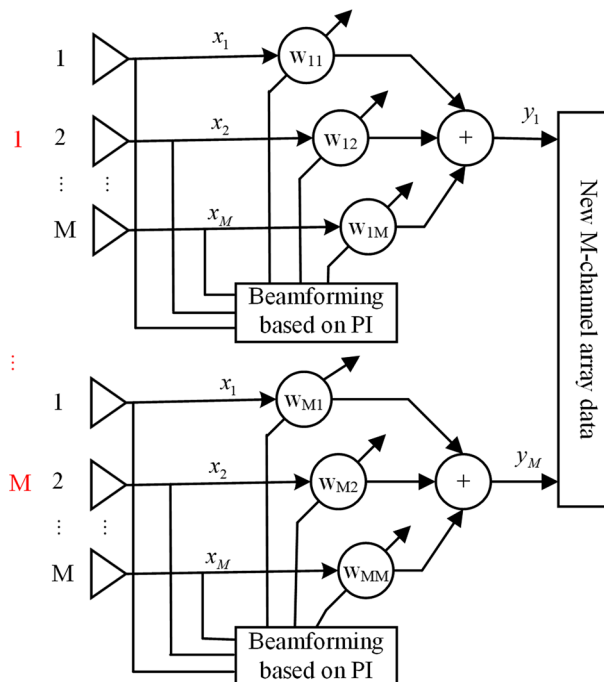

Fig. 2 Flow chart of the parallel PI algorithm

We derive the new array signal obtained by the M-line parallel PI algorithm as a matrix form

$$\mathbf{Y} = \mathbf{A}_k \mathbf{S} + \mathbf{N}_y \tag{11}$$

where $\mathbf{N}_y = [\mathrm{N}_{y1}, \mathrm{N}_{y2}, ..., \mathrm{N}_{yM}]^T$ is an $\mathrm{M} \times \mathrm{T}$ additive white Gaussian noise matrix with zero mean and σ_n^2 variance, and $\mathbf{N}_{ym}$ is the noise received by the mth antenna. The sparse signal $\mathbf{S}$ contains the angle of the desired signal. Remarkably, DOA estimation is the process of reconstructing signal $\mathbf{S}$ by using the new array signal $\mathbf{Y}$ and steering matrix $\mathbf{A}_k$. Therefore, we can determine the DOA estimation of the desired signal according to the number of nonzero elements in $\mathbf{S}$. Equation (11) can be expressed as a l_0-norm model, but the l_0-norm is an NP-hard problem, which can often be expressed as a l_1-norm model. Therefore, Eq. (11) can be expressed as

$$\min \|\mathbf{Y} - \mathbf{A}_k \mathbf{S}\|_F^2 + h\left\|\mathbf{S}^{l2}\right\|_{l_1} \tag{12}$$

where h is the regularization parameter, which is affected by noise. $\mathbf{S}^{l2}$ is the l_2-norm of each row in the matrix $\mathbf{S}$. $||\mathbf{Y}\text{-}\mathbf{A}_k\mathbf{S}||2$ $\mathrm{F} = ||\mathrm{vec}(\mathbf{Y} - \mathbf{A}_k\mathbf{S})||2$ l_2 is used to straighten matrix $\mathbf{Y} - \mathbf{A}_k\mathbf{S}$ by the matrix vec operator and calculate the l_2-norm. To reduce the calculation, the array signal can be sparsely represented as [22]

$$\min \|\mathbf{Y}_{svw} - \mathbf{A}_{kw}\mathbf{S}_{sv}\|_F^2 + h\left\|\mathbf{S}^{l2}\right\|_{l_1} \tag{13}$$

where $\mathbf{Y}_{svw} = \mathbf{R}_y^{-1/2}\,\mathbf{Y}_{sv}$, $\mathbf{A}_{kw} = \mathbf{R}_y^{-1/2}\,\mathbf{A}_k$, $\mathbf{S}_{sv} = \mathbf{S}\mathbf{V}_y\mathbf{D}_{yk}$, $\mathbf{R}_y$ is the covariance matrix of $\mathbf{Y}$, $\mathbf{Y}_{sv} = \mathbf{Y}\mathbf{V}_y\mathbf{D}_{yk}$ is the dimension reduction matrix after the singular value decomposition of $\mathbf{Y}$, $\mathbf{V}_y$ is a $\mathrm{T} \times \mathrm{T}$ dimensional right singular value matrix after the singular value decomposition of $\mathbf{Y}$, $\mathbf{D}_{yk} = [\mathbf{I}_{yk}, \mathbf{0}]$, $\mathbf{I}_{yk}$ is a $\mathrm{K} \times \mathrm{K}$ dimensional identity matrix, and $\mathbf{0}$ is a $\mathrm{K} \times (\mathrm{T} - \mathrm{K})$ dimensional zero matrix.

3.2 Weighted l_1-norm sparse representation DOA estimation for subspace projections

According to Formula (10), we can estimate the DOA of weak signals under strong interference. However, the l_1-norm will destroy the sparsity of the solution and create more spurious peaks in the spectrum under low SNR, resulting in poor accuracy of weak signals DOA estimation and even failure. To solve this problem, we propose a weighted l_1-norm sparse representation DOA estimation for subspace projection. Since the desired signals, interference signals and noise received in the original array are not correlated with each other, the covariance matrix of the received array signals is expressed as

$$\mathbf{R}_x = E\{\mathbf{X}(t)\mathbf{X}^H(t)\} = \mathbf{R}_s + \mathbf{R}_j + \mathbf{R}_n \tag{14}$$

where $\mathbf{R}_s$, $\mathbf{R}_j$ and $\mathbf{R}_n$ are the covariance matrices of the desired signals, interference signals and noise, respectively. The covariance eigenvalue of the received array signal is decomposed as

$$
\begin{aligned}
\mathbf{R}_x &= \sum_{m=1}^{M} \lambda_m \mathbf{u}_m \mathbf{u}_m^H = \sum_{m=1}^{Q} \lambda_m \mathbf{u}_m \mathbf{u}_m^H + \sum_{m=Q+1}^{K+Q} \lambda_m \mathbf{u}_m \mathbf{u}_m^H \\
&\quad + \sum_{m=K+Q+1}^{M} \lambda_m \mathbf{u}_m \mathbf{u}_m^H, \ \lambda_m (m=1,2,\cdots,M, \lambda_1 > \lambda_2 > \cdots > \lambda_M) \\
&= \mathbf{U}_j \mathbf{\Sigma}_j \mathbf{U}_j^H + \mathbf{U}_s \mathbf{\Sigma}_s \mathbf{U}_s^H + \mathbf{U}_n \mathbf{\Sigma}_n \mathbf{U}_n^H
\end{aligned}
\tag{15}
$$

where $\lambda_m (m=1,2,\ldots,M, \lambda_1 > \lambda_2 > \ldots > \lambda_M)$ is the M eigenvalue of $\mathbf{R}_x$, and $\mathbf{u}_m$ is the eigenvector. $\sum_j = \mathrm{diag}\{\lambda_1, \lambda_2, \ldots, \lambda_Q\}$, $\sum_s = \mathrm{diag}\{\lambda_{Q+1}, \lambda_{Q+2}, \ldots, \lambda_{Q+K}\}$ and $\sum_n = \mathrm{diag}\{\lambda_{Q+K+1}, \lambda_{Q+K+2}, \ldots, \lambda_M\}$ are eigenmatrices of the interference signals, desired signals and noise, respectively. $\mathbf{U}_j = \mathrm{span}\{u_1, u_2, \ldots, u_Q\}$, $\mathbf{U}_s = \mathrm{span}\{u_{Q+1}, u_{Q+2}, \ldots, u_{Q+K}\}$, and $\mathbf{U}_n = \mathrm{span}\{u_{Q+K+1}, u_{Q+K+2}, \ldots, u_M\}$ are the interference subspace, desired signal subspace and noise subspace, respectively. Since the eigenvalues of the strong interference are much larger than desired signal, we can select the eigenvector $\mathbf{U}_j$ after selecting the eigenvalue. Therefore, the orthogonal complement space of the interference subspace is

$$
\mathbf{U}_j^{\perp} = \mathbf{I} - \mathbf{U}_j \mathbf{U}_j^H
\tag{16}
$$

We project the array data onto this space to obtain the signal after suppressing interference

$$
\mathbf{z} = \mathbf{U}_j^{\perp} \mathbf{X}
\tag{17}
$$

In the l_1-norm sparse representation DOA estimation algorithm, the l_1-norm is used to replace the l_0-norm. There are only 0 or 1 in the l_0-norm model, and their contributions to the objective function are equal [23]. The l_1-norm model represents the minimum modulus, where the large number is the large modulus value and the small number is a small modulus value in **S**. To make the contribution of **S** to the objective function equal and the l_1-norm closer to the l_0-norm, a small weight punishment is applied to the large modulus, and a large weight punishment is applied to the small modulus in **S**, thus the reconstructed signal can obtain the same constraint. Therefore, **S** needs to be weighted so that the large modulus in Formula (13) is multiplied by the small weight, and the small modulus is multiplied by the large weight. The signal obtained by Formula (17) is used as the input to obtain the quotient of the l_2-norm of the products of the direction vector with the noise subspace and the signal subspace. The weighted value of the l_1-norm under a strong interference signal is

$$
w_{zi} = \left\| \mathbf{E}_{zn}^H \mathbf{b}(\theta_i) \right\|_2 \big/ \left\| \mathbf{E}_{zs}^H \mathbf{b}(\theta_i) \right\|_2
\tag{18}
$$

where $\mathbf{b}(\theta_i)$ is the steering vector, $\mathbf{E}_{zn}$ is the noise subspace and $\mathbf{E}_{zs}$ is the desired signal subspace. The weighted matrix is expressed as

$$
\mathbf{W}_z = \mathrm{diag}\{w_{zi}\}
\tag{19}
$$

Substituting Formula (19) into Formula (13), the weighted l_1-norm sparse representation of the array signal can be derived as

$$\min \|\mathbf{Y}_{svw} - \mathbf{A}_{kw}\mathbf{S}_{sv}\|_F^2 + h\left\|\mathbf{W}_z\mathbf{S}^{l_2}\right\|_{l_1} \tag{20}$$

Formula (20) is solved by the following second-order cone programming problem

$$
\begin{aligned}
&\min p + hq \\
&s.t. \|\mathbf{Y}_{svw} - \mathbf{A}_{kw}\mathbf{S}_{sv}\|_F^2 \le p \\
&\left\|\mathbf{W}_z\mathbf{S}^{l_2}\right\|_{l_1} \le q
\end{aligned}
\tag{21}
$$

The DOA estimation can be obtained by optimizing **S** from Formula (21). The detailed steps are as follows:

(1) According to the PI adaptive beamforming algorithm, y_1 is calculated from the original received array signal in Formula (10).
(2) The proposed parallel algorithm is used to calculate $\mathbf{y}_2$, $\mathbf{y}_3$, …, $\mathbf{y}_M$, and construct a new array signal **Y** after suppressing strong interference.
(3) The new array signal **Y** is converted into Formula (13) according to the sparse representation model.
(4) The original received array signal is projected onto the subspace, and the weighted matrix $\mathbf{W}_z$ is obtained from Formulas (18), (19).
(5) The DOA estimation is obtained from Eq. (21) using second-order cone programming.

4 Results and discussion

Since the UAV video signal works in the ISM frequency band with complicated electromagnetic environments, WiFi is the most common interference source. In this section, WiFi is used as the interference signal, and the UAV video signal is considered the desired signal for the simulation and experiment. In the simulation, the performance of the proposed algorithm is verified by comparison with the JJM algorithm, ENS algorithm and EEOI algorithm using high SIR, low SIR, multi strong interference, RMSE and success rate of DOA estimation under different SIRs or snapshots. In the experiment, we demonstrate the DOA estimation performance of a UAV video signal and a strong WiFi interference in different algorithms.

Table 1 Simulation parameters

Simulation parameters	WiFi	UAV video signal
Number of symbols	6	10
Number of subcarriers (N_c)	64	256
Number of effective subcarriers (N_m)	52	192
Effective symbol time (T_u (us))	3.2	12.8
Cyclic prefix time (T_g (us))	0.8	3.2
Subcarrier bandwidth (Δf(KHz))	312.5	78.125

4.1 Simulation results and discussion

WiFi and UAV video signals are based on an orthogonal frequency division multiplexing (OFDM) modulation scheme with a 20 MHz bandwidth covering frequencies between 2430 and 2450 MHz. As shown in Table 1, WiFi includes 6 OFDM symbols, and each symbol is composed of 64 subcarriers and 52 effective subcarriers. The bandwidth of the subcarrier is 312.5 kHz, and the effective symbol time and the cyclic prefix time are 3.2 μs and 0.8 μs, respectively. While the UAV video signal is composed of 10 OFDM symbols, in which each symbol includes 256 subcarriers and 192 effective subcarriers. The subcarrier bandwidth is 78.125 kHz, with the effective symbol time and the cyclic prefix time being 12.8 μs and 3.2 μs, respectively. A uniform linear array with 8 omnidirectional antennas spaced at half-wavelength (0.06 m) is considered, and the array received signal is added with white Gaussian noise. In the proposed algorithm, the
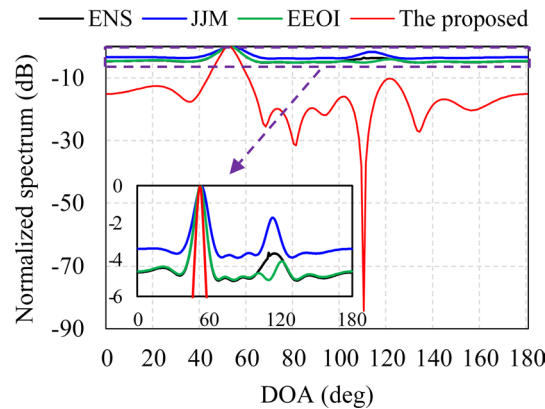

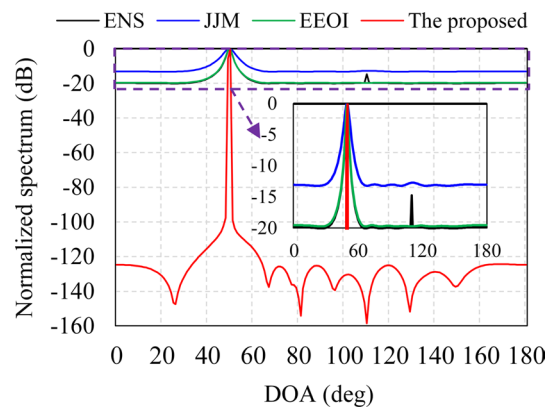**Fig. 3** Normalized spectrum when SIR = − 50 dB

Fig. 4 Normalized spectrum when SIR = − 15 dB

Table 2 DOA estimates in Figs. 2 and 3

SIR (dB)	ENS	JJM	EEOI	Proposed method
− 15	50°	50°	50°	50°
− 50	53°	53°	52°	52°

regularization parameter is $h = 2.7$, and the angle grid is searched in a range of 0° to 180° with 1° intervals.

Simulation 1 Weak signal DOA estimation under high/low SIR.

This simulation compares the DOA estimation performance of the four algorithms at high SIRs and low SIRs. Assume that the angle of WiFi is 110°, and the SNR is 30 dB. The angle of the UAV video signal is 50°, and the SNR is -20 dB (SIR $= -50$ dB) or 15 dB (SIR $= -15$ dB). The number of snapshots is set as 3840. Two scenarios with different levels of SIR are considered herein. Figure 3 shows the normalized spectrum when SIR $= -50$ dB, while Fig. 4 depicts the normalized spectrum when SIR $= -15$ dB. Table 2 presents the estimated results of these two cases. It is seen that when SIR $= -50$ dB or SIR $= -15$ dB, the four algorithms can eliminate the influence of strong interference and estimate the DOA of the weak signal, but the average noise spectrum value of the other three algorithms is much larger than that of the proposed algorithm. When the SIR is low, the average noise spectrum value is approximately -15 dB in the proposed algorithm, and a deep null will be formed at the strong interference. The average noise spectrum values of the other three algorithms are approximately -3.4 dB (JJM), -4.7 dB (ENS), and -4.6 dB (EEOI). Their interference suppression is insufficient, which will lead to spurious peaks and affect the DOA estimation. When the SIR is high, the average noise spectrum value is approximately -124.8 dB in the proposed algorithm, and the average noise spectrum values are approximately -13 dB (JJM), -19.8 dB (ENS), and -19.5 dB (EEOI) in the other three algorithms, Besides, the ENS algorithm cannot suppress the interference completely and produce spurious peaks. As a comparison, the main lobe is sharper and the average noise spectrum value is lower in the proposed algorithm. As the SNR of the UAV video signal decreases, the suppression effect of the algorithms declines, and spurious peaks are easily generated. However, the proposed algorithm not only suppresses the interference, but also weights the desired signal desired signal. Therefore, there is a larger weight in the direction of the desired signal and the opposite in noise, while the other three algorithms are not weighted.

Simulation 2 RMSE and success rate of DOA estimation with different SIRs.

This simulation compares the DOA estimation accuracy and success rate of the four algorithms under different SIRs. Where the DOA estimation accuracy is represented by RMSE

$$\text{RMSE} = \sqrt{\frac{1}{N_c P} \sum_{n_c=1}^{N_c} \sum_{p=1}^{P} \left(\hat{\theta}_p(n_c) - \theta_p \right)^2} \tag{22}$$

where N_c is the number of Monte Carlo iterations, θ_p is the actual angle of the signal, $\hat{\theta}_p(n_c)$ is the DOA estimate of n_cth Monte Carlo iterations. The success rate of DOA estimation is expressed as

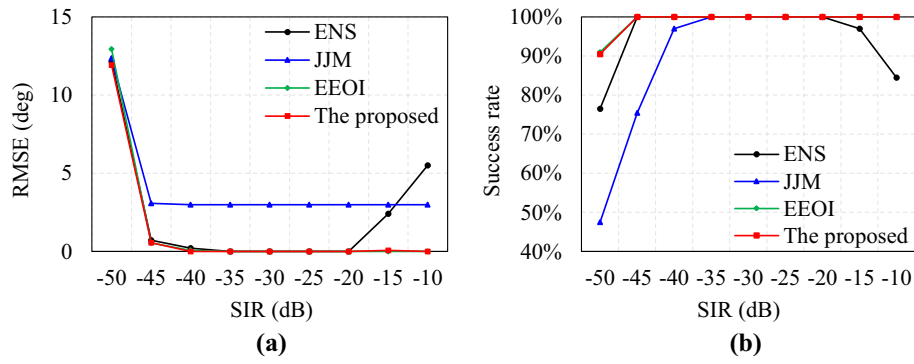$$\text{SR} = \frac{1}{N_c} \sum_{n_c=1}^{N_c} \delta_s \tag{23}$$

Fig. 5 RMSE or success rate of DOA estimation versus different SIRs. **a** RMSE. **b** Success rate
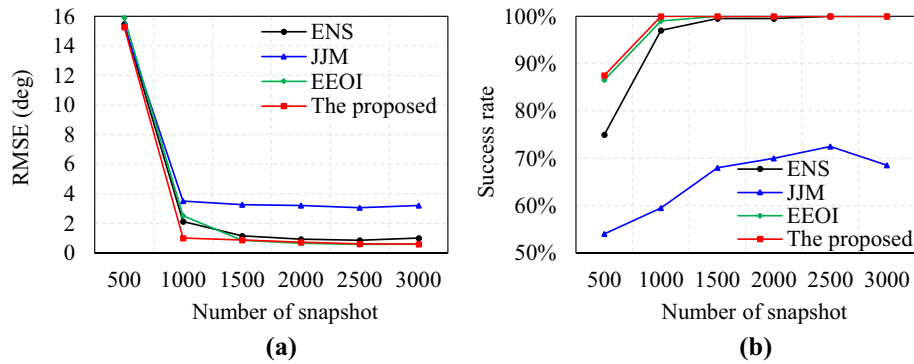

Fig. 6 RMSE or success rate of DOA estimation versus different numbers of snapshots. **a** RMSE. **b** Success rate

where

$$\delta_s = \begin{cases} 1 \; \; if \left| \hat{\theta}_p(n_c) - \theta_p \right| \leq \varepsilon \\ 0 \quad\quad\quad else \end{cases} \tag{24}$$

and ε is a constant.

Assume that the incidence angle of WiFi is 94°, SNR is 30 dB, and the angle of UAV video signal is 80° and the SNR of UAV video signal varies from -20 to 20 dB with step-size of 5 dB. The number of snapshots is set as 3840. We performed 200 Monte Carlo experiments for each SIR and calculated the RMSE and success rate of DOA estimation. Figure 5 presents the relationship between different SIRs vs RMSE and different SIRs vs success rate. We consider the DOA estimation successful when the estimation error is less than or equal to 3°. The proposed algorithm has the same success rate as the EEOI algorithm and has a higher success rate than the other two algorithms. The proposed algorithm has the best DOA estimation accuracy. Specifically, when SIR $= -50$ dB, the DOA estimation accuracy (11.92°) of the proposed algorithm is greater than those of the other three algorithms (ENS: 12.16°, JJM: 12.35°, EEOI: 12.94°). When SIR > -45, the DOA estimation accuracy of the proposed algorithm is the same as that of the EEOI algorithm and greater than those of the other two algorithms. As the SIR increases, the RMSE gradually decreases and tends to be stable,

and the success rate gradually increases and tends to 100% in the proposed algorithm, the JJM algorithm and the EEOI algorithm. However, the accuracy and success rate of DOA estimation first increase and then decrease in the ENS algorithm. This is because as the SIR decreases, the ENS algorithm cannot suppress the interference completely as shown in Fig. 3, or the spurious peaks are greater than the spectrum peaks of the weak signal, resulting in a decrease in accuracy and success rate.

Simulation 3 RMSE and success rate of DOA estimation compared with different number of snapshots.

Assume that the DOA of WiFi is 94°, the SNR = 30 dB, the DOA of the UAV video signal is 80°, and the SNR = −15 dB. The number of snapshots changes from 500 to 3000 in 500 step-size. We performed 200 Monte Carlo experiments for each snapshot and calculated the RMSE and success rate. Figure 6 provides the relationship between different SIRs vs RMSE and different SIRs vs success rate. We also consider the DOA estimation successful when the estimation error is less than or equal to 3°. This shows that the proposed algorithm has the best success rate and accuracy of DOA estimation. As the number of snapshots increases, the RMSE gradually decreases and tends to be stable, and the success rate increases gradually. Since the proposed algorithm is based on the weighted l_1-norm sparse representation DOA estimation, the required number of snapshots is smaller than that of the classic super-resolution algorithm under the same conditions.

Simulation 4 Weak signal DOA estimation under multiple interference.

This simulation compares the DOA estimation performance of four algorithms under two strong interference signals and one weak desired signal. Assume that the DOA of two WiFi and one UAV video signal are 60°, 110° and 80°, respectively. Assume that the SNRs of two WiFi signals are 30 dB and 25 dB, and the SNR of the UAV video signal is 10 dB. Besides, the number of snapshots is set as 3840. Figure 7 depicts the normalized spectrum of the weak signal DOA estimation under two interference signals. The DOA estimations of the proposed algorithm, the ENS algorithm, the EEOI algorithm and the JJM algorithm are 80°, 80°, 80° and 82°, respectively. The average noise spectrum value is approximately −1.3 dB (JJM), −11.6 dB (ENS), −7.7 dB (EEOI) and −117 dB (the proposed algorithm), and spurious peaks appear in the ENS algorithm. The JJM algorithm uses the direction information of the interference signal to construct the blocking matrix, and it reduces the rank of the array matrix. With the increase in the number of interference signals, the rank
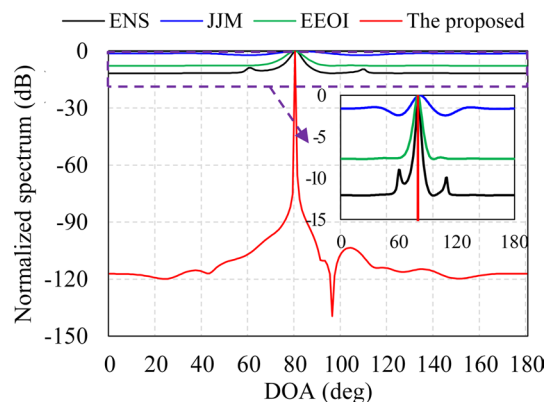

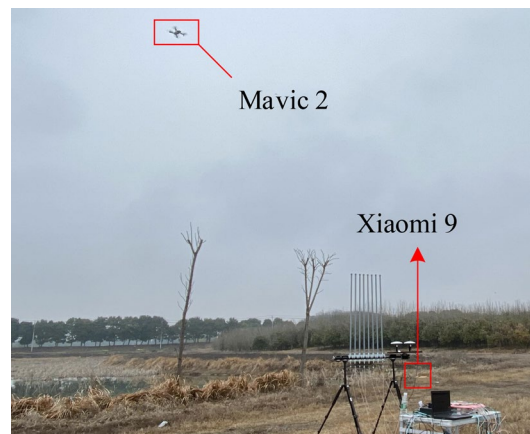**Fig. 7** DOA estimation of a weak signal under two strong interferences

Fig. 8 Photo taken during the real-world experiment of the outdoor scenario
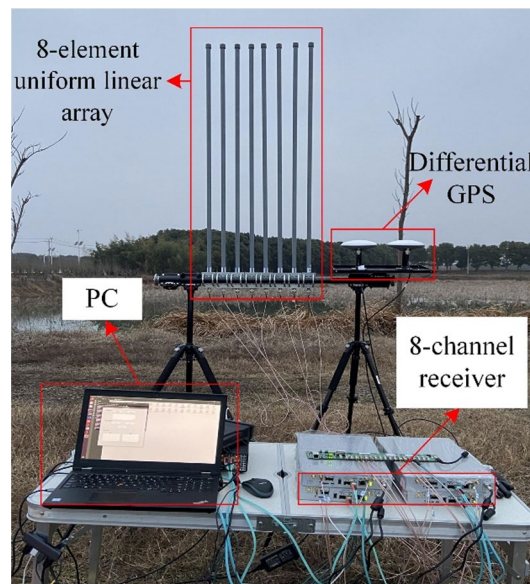

Fig. 9 Photo of the receiving system

of the array matrix decreases. This is equivalent to decreasing the number of array antennas and leads to a decrease in the average noise spectrum value. However, the ENS algorithm and the proposed algorithm do not rely on the rank reduction of the array matrix to suppress strong interference. Moreover, the proposed algorithm adopts the weighted l_1-norm sparse representation for DOA estimation, which has larger weight value in the desired signal direction and a smaller weight value in the noise direction. Therefore, the proposed algorithm has a sharper main lobe and lower average noise spectrum value.

4.2 Experimental results and discussion

In this section, we validate the proposed algorithm through a real-world experiment. Figure 8 illustrates a photo taken in an outdoor experiment next to Liangzi Lake, Jiangxia
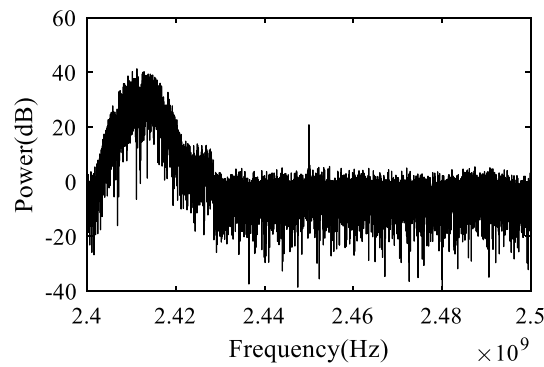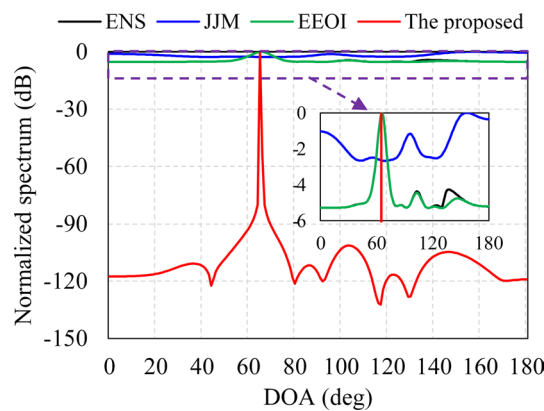
Fig. 10 Spectrum of the received signal

Fig. 11 DOA estimation of the desired signal after suppressing WiFi interference

District, Wuhan, Hubei Province, which includes a DJI Mavic 2 UAV, a Xiaomi 9 mobile phone and a receiving system. The UAV hovers 667 m away from the receiver. Its flight height is 50 m, and the DOA is 62.3°. The mobile phone, which is 12.7 m away from the receiver and 50 cm from the ground, transmits a 20 MHz bandwidth WiFi signal with a frequency range of 2.4–2.5 GHz and a DOA of 128°. Figure 9 presents a photo of the receiving system, which is composed of an 8-element uniform linear array, a SinoGNSS differential GPS, an 8-channel synchronous receiver and a PC. The uniform linear array consists of eight omnidirectional fiberglass dipole antennas with a length of 1.2 m and a gain of 8 dBi, which are fixed on a tripod 150 cm from the ground, and the adjacent element distance is 0.06 m. Differential GPS is used to calibrate north and to calculate the theoretical azimuth with the GPS coordinates at the UAV. The 8-channel synchronous receiver consists of four 2×2 multiple input multiple output (MIMO) USRP N321software-defined radio (SDR) platforms, with an instantaneous bandwidth of 200 MHz covering frequencies between 3 MHz and 6 GHz. Besides, the IQ sampling rate is set as 100 MHz.

Figure 10 displays the spectrum of the received signals. The WiFi signal has a 20 MHz bandwidth covering frequencies between 2402 and 2422 MHz, and the frequency range of the UAV video signal is 2408–2428 MHz. Figure 11 shows that the WiFi amplitude is greater than that of the UAV video signal and the UAV video signal is covered by WiFi. In the algorithm, the number of snapshots is 10000, the regularization parameter is $h = 2.7$, and the angle grid is searched in the range of 0° to 180° with 1° step-size. Figure 11

provides the DOA estimation of the desired signal after suppressing WiFi interference. This shows that the JJM algorithm has many spurious peaks and is sensitive to the angle of the interference signal, which indicates that it is unable to estimate the DOA effectively. The proposed algorithm shows that the DOA estimation is 65°, which is more accurate than that of the other two algorithms (66°). There are many spurious peaks observed in the other two algorithms. The proposed algorithm presents the best performance, with a sharper main lobe and lower average noise spectrum value than other algorithms.

5 Conclusion

This paper investigates the DOA estimation problem of UAV video signals affected by strong WiFi, Bluetooth and other interference signals in complicated electromagnetic environments. A novel DOA estimation based on weighted l_1-norm sparse representation under strong interference is proposed. First, a parallel adaptive beamforming algorithm based on PI is used to suppress strong interference and from new array data, and a weighted matrix is obtained according to the optimized subspace algorithm of subspace projection. Then, the weighted l_1-norm sparse representation DOA estimation is formed by the weighted matrix and new array data. The proposed algorithm combines the advantages of sparse representation DOA estimation with fewer snapshots, a lower average noise spectrum value and higher precision of super-resolution algorithm. In the field experiment, a strong WiFi source is taken as interference for the simulation and experiment. The simulated results show that the proposed algorithm has fewer snapshots, a higher DOA estimation accuracy and success rate, sharper main lobe and lower average noise spectrum value. To demonstrate these results, experimental results also indicate that the proposed algorithm shows better DOA estimation performance than other algorithms. This proves that the proposed algorithm can be used for the DOA estimation of UAV video signals under strong WiFi interference in complicated electromagnetic environments, which has important value and consequences for improving the weak target detection ability. In addition, the proposed algorithm is also suitable for the DOA estimation of weak signals when other interference signals exist in the actual environment, such as the DOA estimation of a 5G signal.

Abbreviations

DOA	Direction of arrival
UAV	Unmanned aerial vehicle
PI	Power inversion
OFDM	Orthogonal frequency division multiplexing
ISM	Industrial, scientific and medical
JJM	Jamming jam method
MUSIC	Multiple signal classification
ENS	Extended noise subspace
EEOI	Elimination of the eigenvectors of interference
SIR	Signal-to-interference ratio

Author contributions
SX and MZ designed the proposed framework; MZ performed the simulations and experiments; SX administrated the project; MZ wrote the paper; All authors read and approved the final manuscript.

Availability of data and materials
The authors state the data availability in this manuscript.

Declarations

Ethics approval and consent to participate
Not applicable.

Consent for publication
Not applicable.

Competing interests
The authors declare that there is no conflict of interest regarding the publication of this paper.

References

1. H. Ullah, M. Abu-Tair, S. Mcclean et al., Connecting disjoint nodes through a UAV-based wireless network for bridging communication using IEEE 802.11 protocols. EURASIP J. Wire. Commun. Netw. **2020**, 142 (2020)
2. G. Yang, X. Shi, L. Feng et al., CEDAR: a cost-effective crowdsensing system for detecting and localizing drones. IEEE Trans. Mob. Comput. **19**(9), 2028–2043 (2020)
3. E. Martins, E. Fatih, K.A. Chethan et al., Detection and classification of UAVs using RF fingerprints in the presence of Wi-Fi and bluetooth interference. IEEE Open J. Commun. Soc. **1**, 60–76 (2019)
4. M. Zuo, S. Xie, X. Zhang et al., Recognition of UAV video signal using RF fingerprints in the presence of WiFi interference. IEEE Access **9**, 88844–88851 (2021)
5. T. Xing, W. Roberts et al., Sparse learning via iterative minimization with application to MIMO radar imaging. IEEE Trans. Signal Process. **59**(3), 1088–1101 (2011)
6. L. Yan, P. Addabbo, C. Hao et al., New ECCM techniques against noiselike and/or coherent interferers. IEEE Trans. Aerosp. Electron. Syst. **56**(2), 1172–1188 (2019)
7. L. Yan, P. Addabbo, Y. Zhang et al., A sparse learning approach to the detection of multiple noise-like jammers. IEEE Trans. Aerosp. Electron. Syst. **56**(6), 4367–4383 (2020)
8. A. Olfat, S. Nader-Esfahani, A new signal subspace processing for DOA estimation. Signal Process. **84**(4), 721–728 (2004)
9. J. Li, P. Stoica, Efficient mixed-spectrum estimation with applications to target feature extraction. IEEE Trans. Signal Process. **44**(2), 281–295 (1996)
10. J. Tsao, B.D. Steinberg, Reduction of sidelobe and speckle artifacts in microwave imaging: the CLEAN technique. IEEE Trans. Antennas Propag. **36**(4), 543–556 (1988)
11. H. Chen, H. Su, A new approach to estimate DOA in presence of Strong jamming/signal suppression. Acta Electron. Sin. **34**(3), 530–534 (2006)
12. W. Dong, Research on the DOA estimation algorithm of weak signal under strong interference. Dissertation, Harbin Inst. of Technol. 2013 (2013)
13. J. Mei, J. Hui, Y. Wang et al., Designing null-forming weights based on Bartlett beam forming. J. Harbin Eng. Univ. **29**(12), 1315–1318 (2008)
14. H. Dong, T. Xu, C. Wang, Two-dimensional weak signal DOA estimation based on corrected projection jam method in the presence of strong interference. J. Signal Process. **29**(2), 221–227 (2013)
15. J. Zhang, G. Liao, J. Zhang, DOA estimation based on extended noise subspace in the presence of strong signals. Syst. Eng. Electron. **31**(6), 1279–1283 (2009)
16. B. Lin, G. Hu, H. Zhou et al., DOA estimation method of weak signal under the compound background of strong interference and colored noise. Int. J. Antennas Propag. (2022). https://doi.org/10.1155/2022/3949988
17. J. Gong, S. Lou, Y. Guo, DOA estimation method of weak sources for an array antenna under strong interference conditions. Int. J. Electron. **105**(11), 1934–1944 (2018)
18. L. Yang, Y. Yang, J. Zhu, Source localization based on sparse spectral fitting and spatial filtering. OCEANS 2016 MTS/IEEE Monterey Conference (2016), p. 1–4.
19. Y. Yang, Y. Zhao, L. Yang, Wideband sparse spatial spectrum estimation using matrix filter with nulling in a strong interference environment. J. Acous. Soc. Am. **143**(6), 3891–3898 (2018)
20. M. Budsabathon, Y. Hara, Optimum beamforming for pre-FFT OFDM adaptive antenna array. IEEE Trans. Veh. Technol. **53**(4), 945–955 (2004)
21. A.B. Gershman, U. Nickel, Adaptive beamforming algorithms with robustness against jammer motion. IEEE Trans. Signal Process. **45**(7), 1878–1885 (1997)
22. M. Zuo, S. Xie, X. Zhang et al., DOA Estimation Based on weighted l1-norm sparse representation for low SNR scenarios. MDPI Sens. **21**(13), 4614 (2021)
23. X. Xu, X. Wei, Z. Ye, DOA estimation based on sparse signal recovery utilizing weighted-norm penalty. IEEE Signal Process. Lett. **19**, 155–158 (2012)

Publisher's Note

Springer Nature remains neutral with regard to jurisdictional claims in published maps and institutional affiliations.